

Development of a low invasive FBG based temperature and strain sensor for aerospace systems management

Original

Development of a low invasive FBG based temperature and strain sensor for aerospace systems management / Aimasso, A.; Bertone, M.; Ferro, C. G.; Maggiore, P.; Dalla Vedova, M. D. L.. - In: JOURNAL OF PHYSICS. CONFERENCE SERIES. - ISSN 1742-6588. - 3063:(2025). (32nd A.I.VE.LA. Annual National Meeting 2024 Forlì (ITA) 19-20 December 2025) [10.1088/1742-6596/3063/1/012008].

Availability:

This version is available at: 11583/3009240 since: 2026-03-25T22:35:33Z

Publisher:

Institute of Physics

Published

DOI:10.1088/1742-6596/3063/1/012008

Terms of use:

This article is made available under terms and conditions as specified in the corresponding bibliographic description in the repository

Publisher copyright

(Article begins on next page)

PAPER • OPEN ACCESS

Development of a low invasive FBG based temperature and strain sensor for aerospace systems management

To cite this article: Alessandro Aimasso *et al* 2025 *J. Phys.: Conf. Ser.* **3063** 012008

View the [article online](#) for updates and enhancements.

You may also like

- [Safety analysis of hoisting points and lifting platform supports in large-span steel structure corridors](#)
Peijun Xie, Pengfei Huang, Jingfeng Li et al.
- [Effect of pulsed laser energy density on the micro-morphology and elemental evolution of oxide film on TC4 surface](#)
Tengchao Liu, Xinqiang Ma, Li Lin et al.
- [Research on adversarial sample attack defense method of automatic modulation recognition system based on deep learning](#)
Hongzhi Liu, Ruonan Jing, Zhiwei Cheng et al.

Development of a low invasive FBG based temperature and strain sensor for aerospace systems management

Alessandro Aimasso¹ , Matteo Bertone¹ , Carlo Giovanni Ferro¹ ,
Paolo Maggiore¹  and Matteo Davide Lorenzo Dalla Vedova^{*1} 

¹ Department of Mechanical and Aerospace Engineering, Politecnico di Torino, Italy

*E-mail: matteo.dallavedova@polito.it

Abstract. In engineering systems development, particularly in mechanical and aerospace applications, there is a great demand for minimally invasive sensors capable of measuring various physical parameters while operating in harsh environments. Optical fiber sensing technology is well-suited to meet the stringent requirements imposed by the operational environment in space. This work describes the conceptualization, development, fabrication and testing phases of an integrated temperature and strain sensor based on Fiber Bragg Grating (FBG) optical sensors. The minimal invasiveness of the final product makes it ideal for a wide range of applications, both for surface measurements and for direct integration into the manufacturing process of the component. The sensor is based on the use of two gratings integrated into different layers of metallic and polymeric materials. This configuration provides a primary FBG directly bonded to the structure, making it sensitive to strain, local temperature and strain induced by temperature changes. Additionally, the proposed design includes a secondary FBG, positioned very close to the first but mechanically isolated from the structure, ensuring a purely thermal measurement. The fabrication of the complete sensor and the subsequent testing phase demonstrated the sensor's high sensitivity along with excellent capability in decoupling thermal and mechanical parameters.

1. Introduction

The activity of systems engineering, especially in the aerospace field, requires access to a large amount of information [1]. These data, essential as input for various types of algorithms (e.g., prognostics or diagnostics) or systems control logics, relies on the quantification of specific physical parameters (temperatures, deformations, friction, compliance, etc.). For this purpose, it becomes crucial to have a network of reliable, integrated, minimally invasive sensors capable of measuring multiple physical parameters using the same hardware [2]. Optical fiber sensors, and specifically FBG sensors, meet this requirement [3]. Furthermore, their use provides a minimally invasive technology that is immune to electromagnetic interference while operating over an extremely wide range of working temperatures. Combined with the ability to host a high number of sensors on the same communication line, optical sensor technology proves to be highly effective even in hostile environments [4].



Consequently, over the last decade, this technology has begun to be studied for industrial applications in various engineering sectors [5-8], also moving to aerospace [9-10]. This paper describes the development and the experimental testing procedure for a minimally invasive sensor capable of simultaneously measuring surface temperature and mechanical deformation induced by applied loads at the same location. Section 2 outlines the physical characteristics of the optical sensors, Section 3 the developed packaging and the tests conducted to verify the sensor's performances and Section 4 summarizes the main results.

2. Optical fiber and sensors

Optical fibers are devices used in numerous engineering sectors, exploiting its capacity of transmitting data but also generating information working as sensor for measuring temperature and deformation. The functioning of the fiber consists in the transmission of electromagnetic waves belonging to a certain band of wavelengths, in general infrared, which represent a signal capable of containing more information than a metal conductor and which is trapped in the innermost layer thanks to the total reflection due to different refractive indices. The Bragg Grating sensor consists of a periodic remodulation of the refractive index of the fiber core, i.e. the innermost layer of the fiber. This remodulation, precisely defined as Bragg grating, has the characteristic of reflecting a specific frequency of the electromagnetic spectrum that passes through the fiber, according to the relation:

$$\lambda_B = 2n_{eff}\Lambda \quad (1)$$

where λ_B is the Bragg frequency is the output of the sensor, n_{eff} is the average value of the refractive index in the sensitive section and Λ is the physical distance between one remodulation and the next. Precisely the dependence of the Bragg frequency on the grating step Λ allows to associate the optical variation with the variation of the physical quantities acting on the sensor:

$$\Delta\lambda = K_T\Delta T + K_\epsilon\Delta\epsilon \quad (2)$$

Finally, the *interrogator* is the instrument used for collecting data. It generates the light beam sent to the fibers to which it is connected and, at the same time, quantify the wavelengths reflected by each grating. In this work, a Smart Scan interrogator model produced by Smart Fiber was used, equipped with 4 communication channels and capable of detecting up to 64 sensors simultaneously.

3. Sensor development and test campaign

The experimental activity that led to the creation and testing of the prototype was divided into 3 fundamental parts:

- Verification of the superposition principle of thermal and mechanical effects on FBG optical sensors;
- Development of the complete sensor geometry;
- Performance verification of the developed sensor.

In this chapter, the above mentioned phases are analyzed in details.

3.1 Verification of thermo-mechanical decoupling sensors capability

Considering the response of the FBG sensor, it is known how the instrumentation is capable of measuring a purely optical output even under varying thermal and mechanical stresses. For this purpose, it is crucial to develop a measurement system capable of separating thermal contributions from mechanical ones, ensuring sensor calibration that provides sufficiently robust data for monitoring potentially complex systems. Additionally, verifying the superposition principle of effects is equally important to apply thermal compensation to mechanical strain sensors. To this end, a preliminary test was conducted to validate the effectiveness of thermal compensation on a sensor simultaneously subjected to mechanical strain and temperature variation. The experimental setup is shown in Figure 1. Two carbon fiber specimens were prepared, each one with an optical fiber containing an FBG sensor bonded to its surface. Both specimens were placed in a climatic chamber: one was subjected to a mechanical load, while the other remained unloaded. The experiment involved, following thermal calibration of the sensors, applying a thermal cycle in the climatic chamber. This thermal cycle was assumed to be perceived identically by both sensors. Additionally, during the temperature variation, a variable mechanical load was applied to the second specimen. The experimental data are shown in Figure 2. At first, the bonding of the optical fiber preserved a linear thermal calibration curve, which is essential for applying the superposition principle. Then, the output trend of the sensor subjected to both types of loads is not directly relatable with the physical parameter of interest. However, as clearly shown in Figure 2/d, after applying the thermal compensation process, the optical data aligned very well with the imposed mechanical load. In From a mathematical point of view, considering the purely thermal sensor, from (2) it is possible to write:

$$\Delta\lambda_{1T} = K_{1T}\Delta T \quad (3)$$

Where K_{1T} is the thermal sensor thermal sensitivity coefficient and $\Delta\lambda_{1T}$ the optical detected variation and then completely due to temperature contribution. So, it can be written:

$$\Delta T = \frac{\Delta\lambda_1}{K_1} \quad (4)$$

Considering also the sensor able to detect mechanical induced loads it is possible to obtain:

$$\Delta\lambda_{2T} = K_{T2}\Delta T = K_{2T} \frac{\Delta\lambda_1}{K_1} \quad (5)$$

where $\Delta\lambda_{2T}$ is the optical variation on the mechanical stressed sensor only due to thermal variation ΔT , written as function of the only thermal sensor parameters, and K_{T2} is the thermal sensitivity coefficient of the second FBG. At this point, set the optical variation of the mechanical stressed sensor as:

$$\Delta\lambda_2 = \Delta\lambda_{T2} + \Delta\lambda_{M2} \quad (6)$$

with

$$\Delta\lambda_{\varepsilon 2} = K_{\varepsilon 2}\Delta\varepsilon \quad (7)$$

the optical variation induced by the mechanical load and $K_{\varepsilon 2}$ the relative mechanical sensitivity coefficient is obtained:

$$\Delta\lambda_2 = K_{2T} \frac{\Delta\lambda_1}{K_1} + K_{\varepsilon 2}\Delta\varepsilon \quad (8)$$

From (8) the measured strain is calculated:

$$\Delta\varepsilon = \frac{\Delta\lambda_2 - K_2 T \frac{\Delta\lambda_1}{K_1}}{K\varepsilon_2} \quad (9)$$

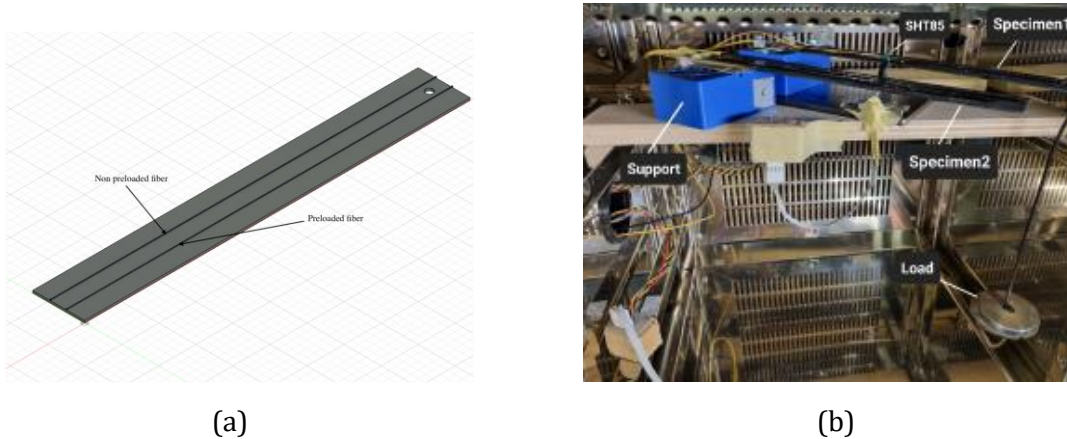


Figure 1. Experimental setup: the single carbon fiber specimen (a) and their arrangement into the climatic chamber (b).

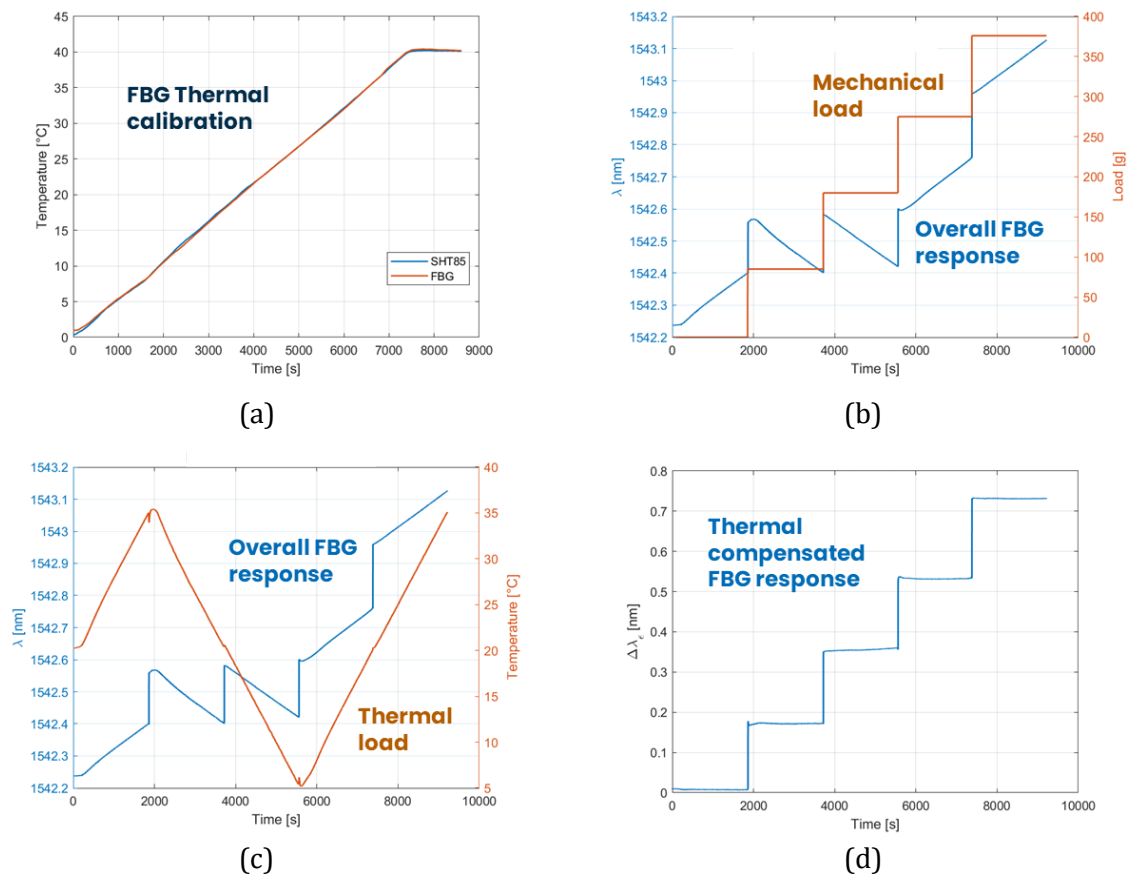


Figure 2. Thermo-mechanical effects decoupling process: thermal calibration (a), application of a mechanical (b) and thermal (c) loads while measuring the overall FBG output, the final thermal compensated FBG curve (d).

Considering equations (4) and (9) and the results demonstrated by this experiment, it is possible to establish the primary physical requirement for the sensor's operation. To achieve an integrated temperature and point-strain sensor, the same approach must be replicated but with a significantly smaller geometry. The adopted approach involves designing an extremely simple rectangular geometry with minimal thickness, capable of providing all the parameters necessary for the local calculation of temperature and strain.

3.2 Sensor design and physical working principle

Figure 3 illustrates the concept and physical setup of the integrated sensor. The setup includes a first FBG sensor, inscribed in an optical fiber and referred to as the mechanical sensor, which is bonded to the measurement surface using an adhesive layer. This adhesive facilitates the transfer of structural deformation to the optical sensor. The adhesive layer is coated with a thin layer of aluminium, which is highly thermally conductive. On top of this aluminium layer, a second FBG sensor, called the thermal sensor, is placed. Unlike the mechanical sensor, it is not glued but simply rests on the metallic surface. This configuration allows the thermal sensor to detect the surface temperature of the entire assembly, leveraging the high thermal conductivity and minimal thermal inertia of the metallic layer. Additionally, because it is only loosely resting on the metal surface, the thermal sensor remains unaffected by mechanical deformation of the substrate, avoiding any deformation induced by structural strain. The only constraint applied to the optical fiber is at the edges of the metallic layer, where an adhesive edge secures the FBG in position.

This adhesive edge not only anchors the thermal fiber but also encapsulates the thermal FBG with an insulating polymer layer. The layer minimizes the influence of convective effects and environmental boundary conditions on the sensor's measurements. Furthermore, if implemented with a proper hermetic adhesion technique, this external layer enables the total lamination of the sensor, given the minimal thickness of the assembly (less than 1 mm). Figure 4 shows the first prototype developed at the Polytechnic University of Turin. This prototype combines high manoeuvrability, thanks to the protection of the optical fibers within an external sheath, with remarkable versatility and minimal invasiveness due to its compact dimensions.

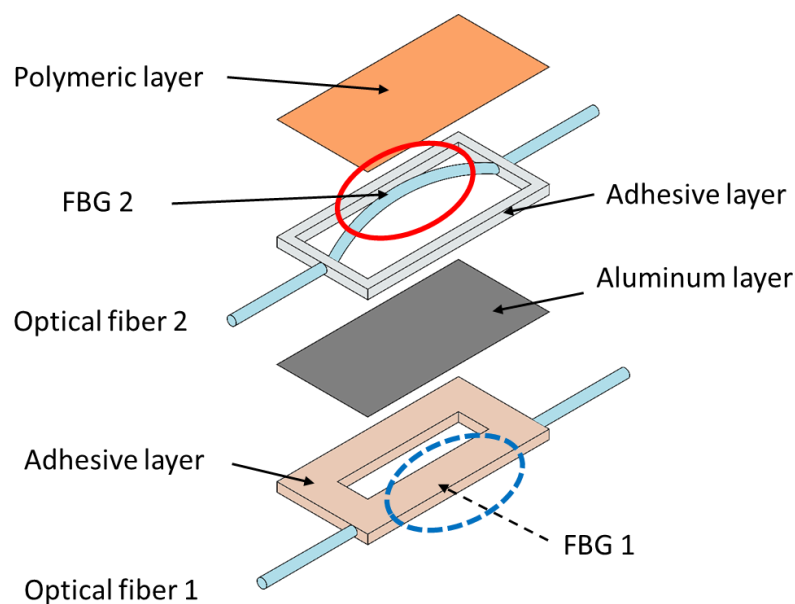


Figure 3. Assembly CAD of the developed sensor. The different layers are clearly viewable.

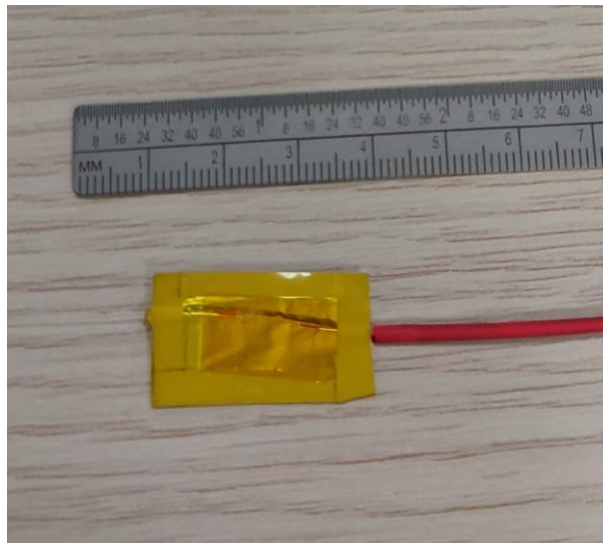


Figure 4. Final assembly of the first prototype. Even without an industrial approach, the minimal invasiveness is perceptible.

3.3 Sensor calibration

Following the development of the first prototype, an initial testing campaign was conducted to calibrate and verify the sensor's functionality based on the proposed design concept. Specifically, Figure 5 illustrates the setup for thermal calibration, as mechanical calibration had already been performed earlier. The experimental setup involved the development of a second prototype, which included a type-T thermocouple placed near the FBG sensor. The testing campaign was conducted using a climatic chamber, subjecting the sensor to a repeated thermal cycle consisting of several temperature steps. Each thermal step involved maintaining a constant temperature value for 30 minutes, during which the average temperature and corresponding average wavelength were recorded. The cycles were repeated 10 times to calculate the uncertainty margin on the calibration curve $w(T)$. The calibration process was carried out using two different FBG sensors. The first sensor was inscribed in a polyacrylate recoated fiber with a visible discontinuity in the coating at the sensor zone. The second FBG was inscribed in a polyimide-coated fiber without noticeable discontinuities in the sensor area. As shown in Figure 6, the first case resulted in a piecewise linear calibration curve, while the second case produced a fully linear calibration curve. Although a detailed analysis of the causes is beyond the scope of this work, a piecewise linear behaviour had been observed in a previous testing campaign for space applications. For operational simplicity, the polyimide sensor was chosen due to its straightforward linearization across the entire thermal range considered.



Figure 5. FBG and thermocouple detail during thermal calibration process

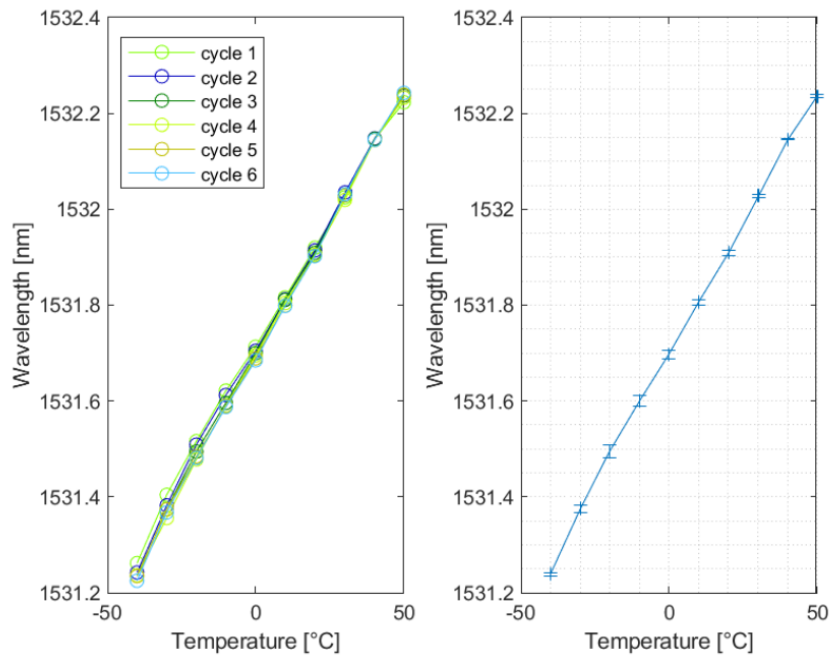
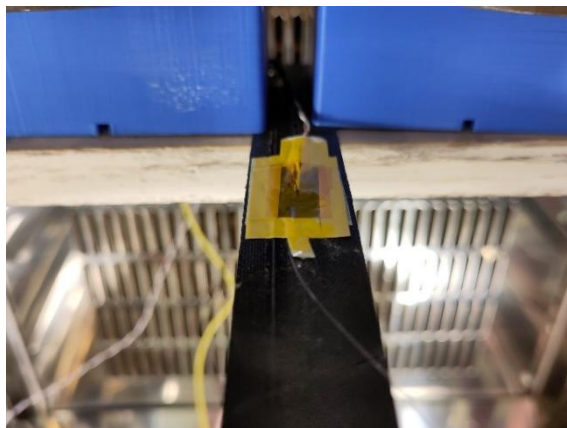


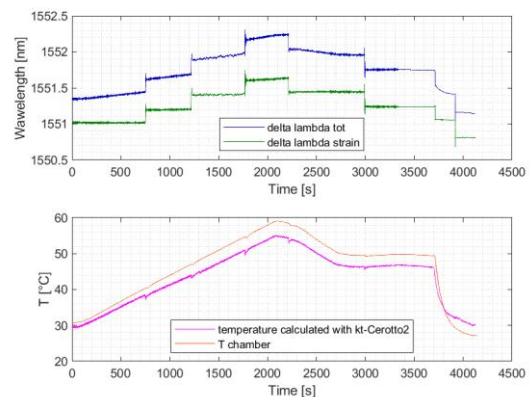
Figure 6. FBG thermal calibration output

3.4 Thermo-mechanical decoupling test

After completing the calibration process, the sensor was mounted on a specimen fixed at one end and subjected to two test cycles. The first cycle was performed at a constant ambient temperature, applying a progressively increasing mechanical load. As shown in Figure 8, the thermal sensor exhibited constant behaviour, entirely independent of mechanical stresses. Conversely, the mechanical sensor accurately detected the applied load. The same approach was repeated with the sensor subjected to simultaneous thermal and mechanical cycles. As observed in Figure 7, the mechanical sensor’s output, influenced by the thermal transient, was effectively corrected using the thermal sensor, which measured the temperature with high accuracy.



(a)



(b)

Figure 7. Sensor final integration on a specimen inside climatic chamber (a) and data collected during the verification test involving thermal and mechanical loads.

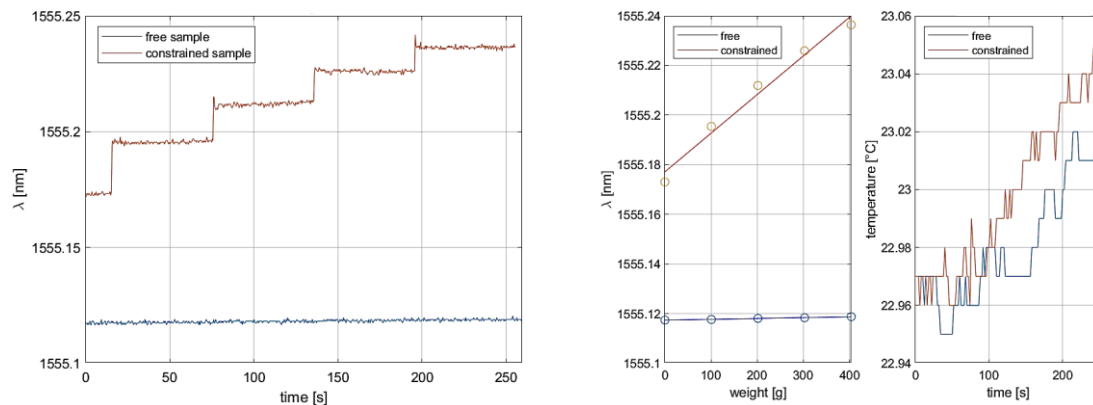


Figure 8. Results of testing involving mechanical loads applied at constant temperature.

4. Conclusions and further developments

The proposed work has achieved highly significant results. A preliminary outcome verified the possibility of applying the principle of superposition of effects to distinguish the thermal contribution from the mechanical contribution in measurements performed using FBG sensors. Based on this consideration, a specific geometry was developed, enabling the creation of a single sensor capable of detecting both temperature and localized strain while ensuring minimal invasiveness and all the physical benefits associated with fiber optics. The sensor demonstrated excellent thermo-mechanical decoupling capability, both in static conditions and during thermal and/or mechanical transients. Thanks to the results obtained in this study, the next step will be to define the sensor's industrialization process to develop an agile, versatile, and plug-and-play instrument suitable for the distributed monitoring of various types of systems.

References

- [1] R. E. Quigley, "More Electric Aircraft," Proceedings Eighth Annual Applied Power Electronics Conference and Exposition, pp. 906–911, 1993.
- [2] Z. Yin, N. Hu, J. Chen, Y. Yang, and G. Shen, "A review of fault diagnosis, prognosis and health management for aircraft electromechanical actuators," IET Electr Power Appl, vol. 16, no. 11, pp. 1249–1272, Nov. 2022,
- [3] A. Behbahani, M. Pakmehr, and W. A. Stange, "Optical Communications and Sensing for Avionics," in Springer Handbooks, Springer Science and Business Media Deutschland GmbH, 2020, pp. 1125–1150.
- [4] S. J. Mihailov, "Fiber Bragg Grating Sensors for Harsh Environments," Sensors, vol. 12, pp. 1898–1918, 2012.
- [5] X. Qiao and Q. Rong, "FBG for Oil and Gas Exploration," Journal of Lightwave Technology, Vol. 37, Issue 11, pp. 2502–2515, vol. 37, no. 11, pp. 2502–2515, Jun. 2019.
- [6] P. Rajeev, J. Kodikara, W. K. Chiu, and T. Kuen, "Distributed Optical Fibre Sensors and their Applications in Pipeline Monitoring," Key Eng Mater, vol. 558, pp. 424–434, 2013.
- [7] C. K. Y. Leung et al., "Review: optical fiber sensors for civil engineering applications".
- [8] A. A. Suryandi, N. Sarma, A. Mohammed, V. Peesapati, and S. Djurović, "Fiber Optic Fiber Bragg Grating Sensing for Monitoring and Testing of Electric Machinery: Current State of the Art and Outlook," Machines, vol. 10, no. 11, p. 1103, Nov. 2022.
- [9] A. Aimasso, A. Facci, M. Bertone, and M. D. L. Dalla Vedova, "Smart Composites Manufacturing and Testing by Insertion of Fiber Bragg Gratings Sensors," 2024.
- [10] D. Wada, H. Igawa, M. Tamayama, T. Kasai, H. Arizono, and H. Murayama, "Flight demonstration of aircraft wing monitoring using optical fiber distributed sensing system," Smart Mater Struct, vol. 28, no. 5, p. 055007, Apr. 2019.